Appl. Phys. B 74, 217–222 (2002)
DOI: 10.1007/s003400200800

Applied Physics B
Lasers and Optics

S. KNAPPE[1,2]
J. KITCHING[2]
L. HOLLBERG[2]
R. WYNANDS[1,✉]

Temperature dependence of coherent population trapping resonances

[1] Institut für Angewandte Physik, Universität Bonn, Wegelerstraße 8, 53115 Bonn, Germany
[2] National Institute of Standards and Technology, 325 S. Broadway, Boulder, CO 80305-3328, USA*

Received: 30 November 2001 /
Published online: 7 February 2002 •

ABSTRACT We measure the properties of coherent population trapping (CPT) resonances in Cs vapor cells as a function of temperature. We expected the CPT signal to increase with higher vapor density, but instead the signal fades away above a certain density. Two possible density-dependent explanations are discussed: spin-exchange collisions, which are found to give no relevant contribution at the temperatures considered here, and increased absorption due to the optical thickness of the vapor. The dependence of the dark-line resonance amplitude as a function of cell temperature can be well represented by a simple model based on the optical thickness of the vapor as a function of temperature.

PACS 42.50.Gy; 32.70.Jz; 32.70.Fw; 32.80.Bx; 42.62.Eh

1 Introduction

Since their first observation in 1976 [1], dark-line resonances based on coherent population trapping (CPT) have found a variety of applications in laser cooling [2] and laser spectroscopy, leading, for instance, to sensitive magnetometers [3] and atomic-frequency references [4]. Steady technical advances have allowed the measurement of very narrow linewidths [5, 6] with high sensitivity in robust and compact setups [7].

The sensitivity of a device based on CPT depends on the density of the atomic medium. This dependence is complicated, however. For optically thin media, a higher density means more atoms interact with the fields, resulting in an increased signal at the CPT resonance. For optically thick cells at higher temperature, the large overall attenuation as well as the spin-exchange collisions between the alkali atoms can decrease the size of the CPT effect substantially. In the case of an alkali atomic vapor at thermodynamic equilibrium in a sealed cell, the density grows exponentially with the cell temperature. Measurements show that when the temperature is increased above a certain point, the amplitude of the dark-line signal decreases and eventually disappears [8]. A similar effect has also been found for a so-called 45° magnetometer based on magnetic resonance with a Zeeman transition in an optically pumped potassium vapor [9]. A temperature-dependent transmission of sodium vapor near a CPT resonance was examined in [10], while in [11] the line narrowing and the influence of the large phase shifts at high density were observed.

We demonstrate here that, for centimeter-scale cells and low laser power, this reduction of signal size at high cell temperature is a result of the increasing optical thickness of the medium and of the fact that spin-exchange collisions play only a small role. While smaller signals result in lower device performance, they can be used to advantage in compact dark-line resonance sensors for mobile applications.

2 Dark-line resonance spectroscopy

Coherent population trapping can be achieved in so-called Λ systems, consisting of two long-lived, low-lying states and an excited state, connected, for example, with the D lines of the alkali atoms. When two near-resonant, phase-stable light fields interact with the two optical transitions from the ground states to the excited state, the atoms are pumped into a coherent dark state if the laser fields' difference frequency exactly equals the ground-state splitting. This dark state is characterized by the presence of a ground-state coherence out of phase with the driving light fields, such that further excitation of the atoms by the light fields is suppressed. The fluorescence intensity is correspondingly reduced, leading to a dark line in the spectrum. Since the resonance width is determined by the lifetime of that coherence, and the coherence can be quite long-lived, very narrow widths can be observed [5, 6].

For compact, simple implementations, the bichromatic light field can be generated by the direct modulation of the injection current of a vertical-cavity, surface-emitting laser (VCSEL) [12]. VCSELs can be manufactured as inexpensive, easy-to-handle devices with low input currents and high modulation bandwidths [13]. Given the limited range of wavelengths where VCSELs are available, the D_2 line of cesium at 852 nm is currently the natural choice of element and excitation wavelength.

✉ Fax: +49-228/73-3474, E-mail: wynands@iap.uni-bonn.de
*Contribution of NIST, an agency of the U.S. Government; not subject to copyright

For Cs, the hyperfine splitting in the ground state is at 9.2 GHz. When the VCSEL current is modulated at one-half this frequency, the dark-line resonance can be prepared by tuning each of the first-order modulation sidebands to the two hyperfine components of the Doppler-broadened optical transition line [12]. Dark-line resonance spectroscopy can then be performed by scanning the two first-order modulation sidebands about their nominal frequency separation of 9.2 GHz. The RF (radio frequency) power coupled into the VCSEL was chosen such that $\approx 60\%$ of the optical power was contained in the first-order sidebands; the remainder resided in the carrier and higher-order sidebands. The power ratio between the blue and red first-order sidebands was approximately 2:1, with the imbalance due to the unavoidable combination of simultaneous frequency and amplitude modulation.

The light was changed to circular polarization and sent through a vapor cell of diameter 20 mm and length 5 mm (alternatively, a cell of length 20 mm was used) and detected with a photodiode (Fig. 1). The resonant laser intensity that resulted in the best signal-to-noise ratio was found to be 50 μW/cm^2 for the beam diameter of 4 mm. The vapor cell contained 5 kPa of neon buffer gas that was added in order to increase the interaction time of the Cs atoms with the laser beam. The cell was surrounded by a magnetic and a thermal shield. A longitudinal magnetic flux density of approximately 4 μT was applied to separate the Zeeman components. In the following, only the central component ("clock transition"), corresponding to the coupling of the ground states $|F = 3, m = 0\rangle$ and $|F = 4, m = 0\rangle$, will be considered.

The cell was heated and the temperature was stabilized to within a few millikelvins. The dark-line resonance was detected by scanning the RF frequency and measuring the transmitted power. In order to increase the signal-to-noise ratio, the RF frequency was modulated at $\omega_m = 2\pi \times 530$ Hz, and the photodiode signal demodulated with a lock-in amplifier. The dc current of the laser was stabilized to the point of minimum noise [14] near the center of the Doppler-broadened absorption peak by modulating it at 10 kHz and demodulating the photodiode signal with a second lock-in amplifier. This choice of operating point also results in symmetric, Lorentzian-like resonance lines [2].

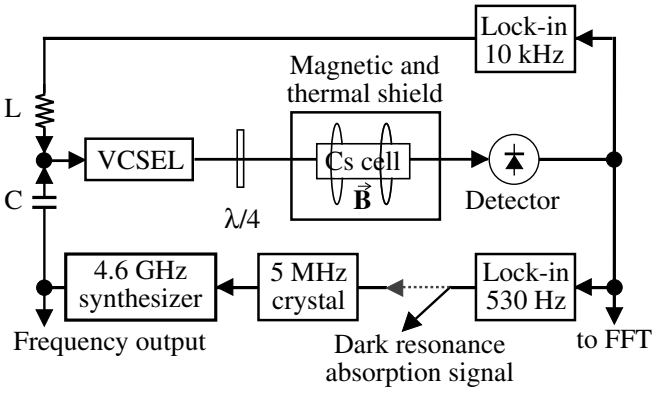

FIGURE 1 Experimental setup. When the switch is closed (*dashed line*), the system works as an atomic-frequency reference, an atomic clock

3 Cell temperature

3.1 *Experimental evidence*

A series of dark-line resonance spectra was measured for various temperatures of the vapor cell. For each measurement point, the cell temperature was allowed at least 2 h to stabilize. The dark-line resonance was then detected by scanning the 4.6-GHz RF frequency, and therefore the difference frequency of the two resonant light fields. Due to the 530-Hz frequency modulation the dark-line spectra contain three contributions, one by the carrier (subscript $j = 0$) and one each by the two first-order sidebands (subscripts $j = \pm 1$). The in-quadrature output, $S(\Delta\omega)$, of the lock-in amplifier as a function of laser difference frequency, $\Delta\omega$, can be written as [15]

$$S(\Delta\omega) \propto [\varphi_{-1}(\Delta\omega) + \varphi_{+1}(\Delta\omega) - 2\varphi_0(\Delta\omega)] \,, \tag{1}$$

where the functions $\varphi_j(\Delta\omega)$ describe the phase shift that each laser frequency component, j, has experienced after transmission through the cell. The phase shifts $\varphi_j(\Delta\omega)$ are proportional to the real part of the complex index of refraction of the medium. Here we assume that the $\varphi_j(\Delta\omega)$ have a dispersion-like Lorentzian shape. These must have the same widths and amplitudes for all j [15]:

$$\varphi_j(\Delta\omega) \propto \frac{\Delta\omega + j\omega_m}{(\Delta\omega + j\omega_m)^2 + \gamma_{CPT}^2} \,. \tag{2}$$

Here γ_{CPT} is the full width at half maximum (FWHM) of the dark-line resonance.

Figure 2 shows the peak-to-peak height of the measured frequency-modulation lineshape as a function of cell temperature. The CPT resonance amplitude increases with temperature up to a certain point and then drops rapidly at higher temperatures, disappearing completely around 65 °C. Since destruction of the ground-state coherence by 9.2-GHz blackbody radiation is completely negligible in this temperature regime, we consider two density-dependent effects that could

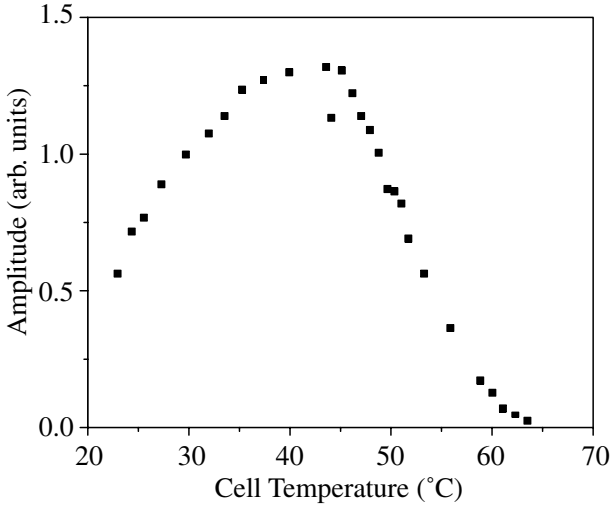

FIGURE 2 Amplitude of the dark-line resonance as a function of vapor cell temperature (resonant light power 37 μW)

be responsible for the observed behavior: spin-exchange collisions and increased absorption in an optically thick vapor. Both will affect the dark-line resonance width and amplitude simultaneously, allowing us to distinguish between the two processes. We will now examine them in turn.

3.2 *Spin-exchange collisions*

Spin-exchange collisions can occur when two alkali atoms collide and exchange spin angular momentum. Both the amplitude and the width of the dark-line resonance depend on the coherence between the two lower states of the Λ system. Spin-exchange collisions destroy this coherence, thereby increasing the width and reducing the amplitude of the resonance. If these collisions were responsible for the decrease in resonance amplitude as seen in Fig. 2, γ_{CPT}, the decay rate of the coherence, should correspondingly be increased significantly.

The contribution of Cs–Cs collisions to the ground-state coherence relaxation rate is proportional to the Cs number density, n_{Cs}, and is given by [16]

$$\Gamma_{\mathrm{Cs-Cs}} = \frac{6I_{\mathrm{N}}+1}{8I_{\mathrm{N}}+4}\bar{v}_{\mathrm{rel}} n_{\mathrm{Cs}} \sigma_{\mathrm{SE}} \,. \tag{3}$$

For cesium, with nuclear spin quantum number $I_{\mathrm{N}} = 7/2$, the spin-exchange cross-section is $\sigma_{\mathrm{SE}} = (2.18 \pm 0.12) \times 10^{-14}\,\mathrm{cm}^2$ [17, 18]. The average relative velocity is given as a function of temperature as $\bar{v}_{\mathrm{rel}} = \sqrt{16 k_{\mathrm{B}} T/\pi m_{\mathrm{Cs}}}$, where m_{Cs} is the Cs atomic mass [19]. The density n_{Cs} increases exponentially with temperature:

$$n_{\mathrm{Cs}} = \frac{p_0}{k_{\mathrm{B}} T} \exp\left(-\frac{T_0}{T}\right) . \tag{4}$$

For cesium the vapor pressure, p_0, at the reference temperature $T_0 = 9132\,\mathrm{K}$ is $1.950 \times 10^9\,\mathrm{Pa}$ for the vapor phase [20].

The spin-exchange cross-section itself is slightly temperature dependent, but the 2% change over 100 K [21] can be neglected. For temperatures near 60 °C, the estimated broadening of the dark line as a result of spin-exchange collisions is 100 Hz FWHM and thus similar in magnitude to the other broadening factors. In the experiment, the width of the resonance remains basically constant or even decreases slightly with temperature. This can be seen in Fig. 3, where the full width of the CPT resonance, γ_{CPT}, (referenced to the full 9.2-GHz frequency splitting and determined by fitting (1) to the experimental lineshape) is shown as a function of cell temperature (solid squares). In the 5-mm-long cell, the width of the CPT resonance is about 700 Hz; the broadening is due mostly to collisional dephasing of the Cs atoms at the cell windows.

To resolve more subtle changes in the width of the resonance, the same measurement was performed in a cell of length 20 mm but otherwise identical. Here the linewidth is reduced by a factor of two (open squares in Fig. 3) because of less-frequent collisions of the atoms with the cell windows. It can be seen more clearly here that the CPT width decreases with cell temperature. A calculation of the expected width due to spin-exchange collisions between the cesium atoms, using (3), is represented by the dashed line. To account for

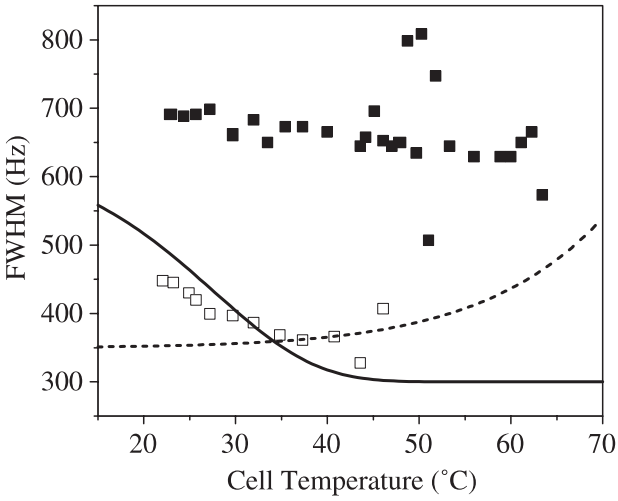

FIGURE 3 Full-width at half maximum (FWHM) of the dark-line resonance as a function of cell temperature in a cell of 5-mm length (*solid squares*) or of 20-mm length (*open squares*), referenced to the full 9.2-GHz hyperfine splitting. *Dashed* and *solid lines* are theoretical predictions for broadening of the dark-line resonance due to spin-exchange collisions and optical density effects, respectively

temperature-independent contributions to the width due to buffer gas and wall collisions, a constant width of 350 Hz was added to the spin-exchange contribution.

Since the Cs-Cs collisions destroy the ground-state coherence, they should decrease the dark-line resonance amplitude and simultaneously broaden it significantly. Obviously, in the range of 40–50 °C, where the dark-line resonance amplitude in Fig. 2 begins to decrease, the spin-exchange contribution to the width is only a few hertz. We can therefore conclude that spin-exchange collisions are not responsible for the reduction in amplitude of the dark-line resonance.

3.3 *Optical-thickness effect*

The remaining possibility to account for the amplitude reduction of the resonance is a strong increase in the absorption coefficient with temperature as the cell becomes optically thick. The width of the dark-line resonance should then be a function of the light intensity at every single position in the light path over the whole cell, with lower local intensities giving rise to narrower local contributions to the overall lineshape due to reduced power broadening. Modelling this behavior is rather complicated because the effects of propagation must be integrated over the length of the cell and, strictly speaking, also over the transverse intensity profile of the laser beam. However, a simple phenomenological model is found to reproduce the disappearance of the dark-line resonance for higher cell temperatures.

To analyze the effects of optical thickness, the absorption coefficient, α, was calculated as a function of temperature. It can be estimated from the transmitted resonant power through the vapor cell if the sideband power is known: only the two first-order sidebands are on resonance, and so only those frequency components can be absorbed. For higher temperatures, the optical absorption saturates at 66%, meaning the fraction of resonant light in the two first-order sidebands is that fraction of the total power.

At optical intensities for which the ground-state level populations are not significantly altered from their equilibrium values, Beer's law is a good approximation. It predicts that this absorbed fraction of the total resonant incident light intensity, I_0, over the cell of length L will depend exponentially on α. α, in turn, is proportional to the atom number density, n_{Cs}, and therefore depends strongly on the temperature of the vapor, according to (4). For the absorbed fraction it follows that

$$1-\frac{I_{\mathrm{trans}}(L)}{I_0} = 1-\exp\left[-\alpha(T)L\right] = 1-\exp\left[\frac{-\vartheta_{\mathrm{abs}}}{T}\exp\left(-\frac{T_0}{T}\right)\right]. \quad (5)$$

The constant ϑ_{abs} includes the proportionality factor between α and n_{Cs}.

Experimental results for the absorbed fraction of resonant light in each sideband are plotted in Fig. 4. The lines in the figure are fits of (5), where ϑ_{abs} is the only fit parameter. For a cesium cell 5-mm long, almost no resonant light is transmitted at temperatures above 55 °C. This suggests that the reduction in amplitude of the resonance at higher temperatures is caused by the vapor becoming opaque.

The amplitude, $h_{\mathrm{CPT}}\left(I_{\mathrm{trans}}(T)\right)$, of the dark-line resonance should thus depend on the intensity of the transmitted light. Although the cesium atom has a rather complex level structure, it was found that it can be described by an effective three-level theory amazingly well [8]. For a closed, symmetric, three-level system, h_{CPT} was derived in [16] to be

$$h_{\mathrm{CPT}} \propto n_{\mathrm{Cs}}\frac{G^2 I_{\mathrm{trans}}^2}{\Gamma^2}\frac{1}{2\Gamma_{12}+G I_{\mathrm{trans}}/\Gamma} \propto \frac{I_{\mathrm{trans}}^2}{I_{\mathrm{S}}+I_{\mathrm{trans}}}. \quad (6)$$

Here $G = g^2/I_{\mathrm{trans}}$, g is the Rabi frequency of the optical excitation, and I_{trans} is the corresponding laser intensity. Γ_{12} and Γ are the decay rates of the ground-state coherence and the optical coherence, respectively. This means that for low intensities, i.e., $I_{\mathrm{trans}} \ll I_{\mathrm{S}} = \Gamma_{12}\Gamma/G$, the amplitude rises quadratically with I_{trans}, whereas at higher intensities it increases proportional to I_{trans} (Fig. 5). The squares are the measured values, while the solid line is a fit of (6) to the data below 70 μW/cm^2. The scaling factor of the amplitude is the only fitted parameter in this case because I_{S} can be obtained from the linewidth data of the same spectra as those underlying Fig. 5 with the help of a relation derived in [2]:

$$\gamma_{\mathrm{CPT}} = 2\Gamma_{12} + (G/\Gamma) I_{\mathrm{trans}}. \quad (7)$$

One finds the best fit to the data points for γ_{CPT} with $I_{\mathrm{S}} = 14(1)\mu\mathrm{W/cm}^2$.

The good agreement between the data and the fit at low intensity in Fig. 5 shows that the numbers derived from the CPT resonance amplitude and width are consistent with each other and with the models (6) and (7). For higher intensities, the width becomes larger than the modulation frequency and the model corresponding to (1) starts to become over-determined because the carrier and sidebands of the 530-Hz modulation are now overlapping completely. For higher modulation frequencies this would happen at higher intensities, but since the optimum operating point of the dark-line spectrometer is at low intensities, the behavior at higher intensities is not of concern here.

One can now try to derive the temperature dependence of the dark-line amplitude by plugging into (6) the measured dark-line amplitude for one fixed temperature, T_{C}, and then scaling it with the temperature-dependent vapor density (4). The result is

$$h_{\mathrm{CPT}}(T) = \varepsilon h_{\mathrm{CPT}}\left(I(T)\right) \times \frac{n_{\mathrm{Cs}}(T)}{n_{\mathrm{Cs}}(T_{\mathrm{C}})} \quad (8)$$

$$= \varepsilon \frac{I_0^2 \exp\left(-\frac{2\vartheta_{\mathrm{CPT}}}{T}\mathrm{e}^{-T_0/T}\right)}{I_S + I_0 \exp\left(-\frac{\vartheta_{\mathrm{CPT}}}{T}\mathrm{e}^{-T_0/T}\right)} \times \frac{T_{\mathrm{C}}}{T}\exp\left(-\frac{T_0}{T}+\frac{T_0}{T_{\mathrm{C}}}\right), \quad (9)$$

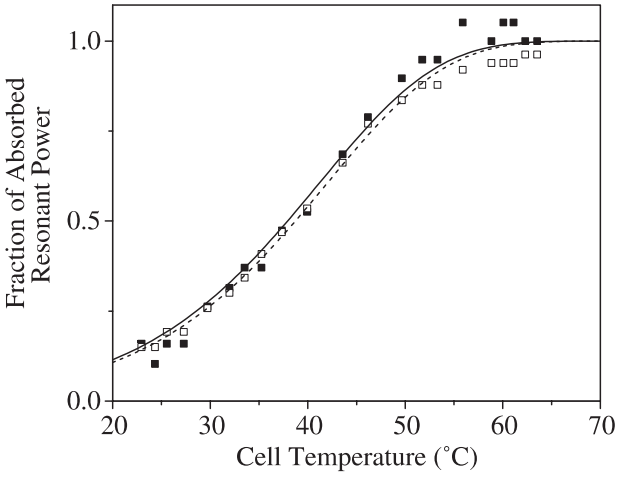

FIGURE 4 Absorbed fraction of resonant laser power in a cell 5-mm long as a function of temperature. *Solid* and *open symbols* represent the measurements for the absorption of the high- and low-frequency first-order sidebands, respectively. *Solid* and *dashed lines* show the fits of (5) to these two sets of data, respectively

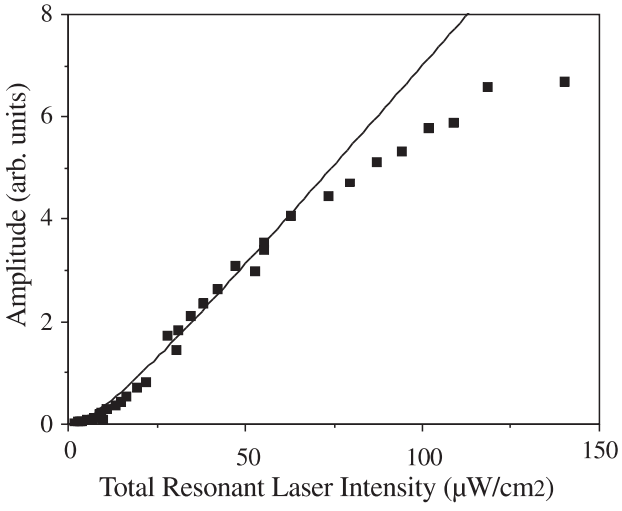

FIGURE 5 CPT amplitude as a function of total resonant laser intensity (*squares*) at a cell temperature of 20.7 °C. The *solid line* is the fit of (6) to the data below 70 μW/cm^2

where I_0 is the resonant intensity incident on the cell. In Fig. 6, the solid lines are obtained with ϑ_{CPT} and the scaling factor ε as the only free parameters. The squares represent the measurements with the 5-mm-long cesium cell. Open symbols correspond to a measurement with total resonant light intensity $I_0 = 122.1\,\mu\mathrm{W/cm^2}$, while for the solid symbols $I_0 = 24.4\,\mu\mathrm{W/cm^2}$ is used. The peculiar shape of the experimental curves is very well represented by the model (9), supporting the proposition that the temperature dependence is essentially an optical-thickness effect.

Additional confirmation can be obtained by varying the cell's length. For each cell length the CPT resonance amplitude should reach a maximum at a temperature corresponding to the same optical thickness. This can clearly be seen in Fig. 6, where the triangles correspond to measurements taken with a cesium cell of length 20 mm, but otherwise identical to the 5-mm long cell. For the short cell, the resonance amplitude is lower for the same optical thickness and intensity because collisions with the windows are more frequent, destroying the coherence and therefore broadening the resonance line.

Table 1 summarizes the various values obtained for ϑ, the proportionality factor between vapor density and absorption coefficient, using the models introduced above. ϑ_{CPT} is the relevant free parameter in (9); $\vartheta_{\mathrm{abs,high}}$ and $\vartheta_{\mathrm{abs,low}}$ were obtained from the fits of (5) by using the data for the absorbed fraction of the upper and lower modulation sidebands, respectively.

Within the measurement uncertainties we find a good agreement between the values for ϑ in each row of the table. Furthermore, we expect the absorption, i.e., ϑ, to be proportional to the length of the cell. The values for the long cell should thus be four times larger than those for the short cell,

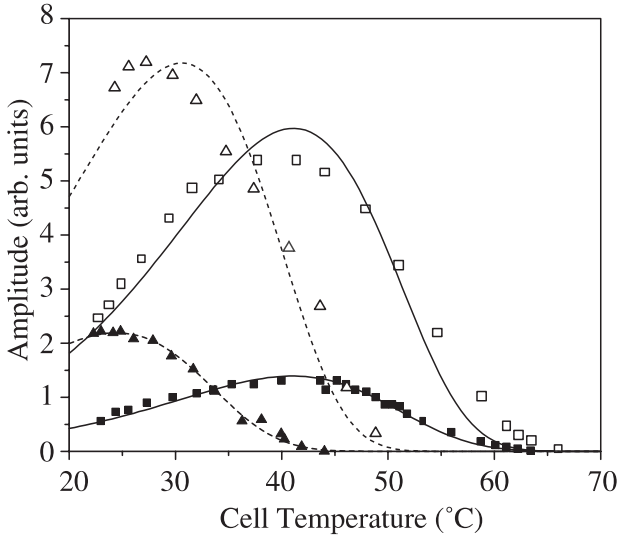

FIGURE 6 Amplitude of the dark-line resonance as a function of vapor cell temperature for a cesium cell containing 5-kPa Ne of 5-mm length (*squares*, *solid lines*) or 20-mm length (*triangles*, *dashed lines*), illuminated with 24.4 $\mu\mathrm{W/cm^2}$ (*solid symbols*) or 122.1 $\mu\mathrm{W/cm^2}$ (*open symbols*) total resonant incident light intensity. Only ϑ_{CPT} and the scaling factor ε are fitted for the lines, representing (9)

Cell	Intensity	ϑ_{CPT} (10^{15} K)	$\vartheta_{\mathrm{abs,\,high}}$ (10^{15} K)	$\vartheta_{\mathrm{abs,\,low}}$ (10^{15} K)
Long	Low	4.2	4.3	4.4
Long	High	2.9	3.4	2.9
Short	Low	0.9	1.2	1.1
Short	High	1.1	1.0	0.9

TABLE 1 Values of the scaling parameter ϑ: ϑ_{CPT} fitted with (9); $\vartheta_{\mathrm{abs,\,high}}$ and $\vartheta_{\mathrm{abs,\,low}}$ taken from the fits to (5) for the blue and red first-order sidebands, respectively

which is approximately the case. Changing the incident laser intensity, in contrast, should not change the absorption coefficient. This is true for the short cell; for the long cell there is a small discrepancy that is not explained by the simple model.

Another check on the consistency of the model involves the width of the CPT resonance, measured as a function of cell temperature (Fig. 3). The solid line is calculated using the measured resonant laser intensities behind the cell and the measured value for the slope G/Γ in (7). A constant width of 300 Hz has been added to represent the temperature-independent contributions, thus allowing for easier comparison with the experimental data. The decrease in linewidth due to reduced power broadening at the higher densities, corresponding to higher cell temperatures, is well represented by the optical-thickness model.

4 Conclusion

In conclusion, the reduction of the dark-line signal amplitude with increasing temperature can be modelled well as an optical-thickness effect. Remarkably, a calculation based on a simple, symmetric three-level system is all that is needed to explain the experimental data. Spin-exchange collisions do not appear to play a role for temperatures below 60°.

For applications where a miniaturized setup is desirable, the shorter vapor column in a small cell would require a higher operating temperature in order to have the same number of atoms participating in the resonance. Fortunately, as was shown here, the reduction in signal size for increasing temperature is not due to spin-exchange collisions, which would have broadened the resonance and therefore reduced the sensitivity of the device. The optical-thickness effect, in contrast, is not a problem for miniaturization, because heating a small cell simply brings up the optical density to the value it had in the optimum case for a longer cell at lower temperature. The higher operating temperature may actually simplify the construction of sensors for in-field applications, because the thermal control system becomes much more efficient when only heating rather than heating and cooling is required over the full range of expected ambient temperatures.

ACKNOWLEDGEMENTS S.K. and R.W. thank the German Academic Exchange Service for support. R.W. gratefully acknowledges additional support by the Deutsche Forschungsgemeinschaft. This work was funded in part by NIST.

NOTE ADDED IN PROOF Very recently we became aware of the article by T. McCelland et al., Phys. Rev. A **33**, 1697 (1986), where for the related case of a microwave resonance experiment on the Cs clock transition a line-narrowing was observed at elevated temperatures, similar to our Fig. 3. Using a different theoretical approach they reached conclusions consistent with ours.

REFERENCES

1 G. Alzetta, A. Gozzini, L. Moi, G. Orriols: Il Nuovo Cim. **36B**, 5 (1976)
2 E. Arimondo: Prog. Opt. **35**, 257 (1996)
3 M. Stähler, S. Knappe, C. Affolderbach, W. Kemp, R. Wynands: Europhys. Lett. **54**, 323 (2001)
4 J. Kitching, S. Knappe, N. Vukičević, L. Hollberg, R. Wynands, W. Weidemann: IEEE Trans. Instrum. Meas. **49**, 1313 (2000)
5 S. Brandt, A. Nagel, R. Wynands, D. Meschede: Phys. Rev. A **56**, R1063 (1997)
6 M. Erhard, S. Nußmann, H. Helm: Phys. Rev. A **62**, 061802(R) (2000)
7 J. Kitching, L. Hollberg, S. Knappe, R. Wynands: Electron. Lett. **37**, 1449 (2001)
8 S. Knappe: Ph.D. thesis, Bonn University (2001)
9 S. Schwarzer: Diplom thesis, Bonn University (2001)
10 S. Baluschev, N. Leinfelder, E.A. Korsunsky, L. Windholz: Eur. Phys. J. D **2**, 5 (1998)
11 M.D. Lukin, M. Fleischhauer, A.S. Zibrov, H.G. Robinson, V.L. Velichansky, L. Hollberg, M.O. Scully: Phys. Rev. Lett. **79**, 2959 (1997)
12 C. Affolderbach, A. Nagel, S. Knappe, C. Jung, D. Wiedenmann, R. Wynands: Appl. Phys. B **70**, 407 (2000)
13 R. King, R. Michalzik, C. Jung, M. Grabherr, F. Eberhard, R. Jäger, P. Schnitzer, K.J. Ebeling: In *Vertical-Cavity Surface-Emitting Lasers II*, ed. by R.A. Morgan, K.D. Choquette. Proc. SPIE **3286**, 64 (1998)
14 J. Kitching, L. Hollberg, S. Knappe, R. Wynands: Opt. Lett. **26**, 1507 (2001)
15 G.C. Bjorklund, M.D. Levenson, W. Lenth, C. Ortiz: Appl. Phys. B **32**, 145 (1983)
16 J. Vanier, A. Godone, F. Levi: Phys. Rev. A **58**, 2345 (1998)
17 W. Happer: Rev. Mod. Phys. **44**, 169 (1972)
18 T.G. Walker, W. Happer: Rev. Mod. Phys. **69**, 629 (1997)
19 J. Vanier, C. Audoin: *The Quantum Physics of Atomic Frequency Standards* (Adam Hilger, Bristol 1989)
20 J.B. Taylor, I. Langmuir: Phys. Rev. **51**, 753 (1937)
21 C.K. Chang, R.H. Walker: Phys. Rev. A **178**, 198 (1969)